Surface Science 260 (1992) 257–266
North-Holland

surface science

Sputtering of silver dimers: a molecular dynamics calculation using a many-body embedded-atom potential

A. Wucher
Fachbereich Physik and SFB 91, University of Kaiserslautern, 6750 Kaiserslautern, Germany

and

B.J. Garrison
Department of Chemistry, Pennsylvania State University, University Park, PA 16802, USA

Received 24 May 1991; accepted for publication 12 July 1991

The ejection of neutral Ag atoms and Ag_2 dimers under 1 keV Ar^+-bombardment of (111)-, (110)- and (100)-silver surfaces was studied by a molecular dynamics simulation using a many-body embedded-atom method (EAM) interaction potential. The absolute dimer yields Y_{Ag_2} as well as the translational and internal energy distributions were calculated using the EAM potential for the description of both the solid and the isolated dimer. Significant differences were found between Y_{Ag_2} obtained for different crystal faces which, however, do not agree with the results of previous studies using additive pair potentials. The calculated translational energy distributions of both atoms and dimers, averaged over the three crystal faces, show good agreement with the corresponding experimental data obtained for a polycrystalline silver surface. The internal state distributions calculated for the sputtered Ag_2 molecules can be fitted by thermal populations revealing vibrational and rotational temperatures of 4200–5800 K and 8500–12300 K, respectively, with the (110)-surface always producing the highest and the (111)-surface the lowest temperatures.

1. Introduction

Throughout the past fifteen years, a considerable amount of both theoretical and experimental work has been devoted to the sputtering of diatomic molecules which has been the subject of several reviews [1–3]. As for the theoretical part, one of the fundamental ways to approach the problem has been to start out from analytical sputtering theory for the ejection of *atoms* and then use statistical models to describe the molecule formation. In this context, in principle two basic ejection mechanisms are generally distinguished in the literature. The direct emission mechanism (DEM) involves a single collision between a moving atom from the collision cascade and a molecule already existing at the surface. Then, if the energy transferred to the center-of-mass exceeds the surface binding energy of the molecule and the relative kinetic energy of the two atoms remains lower than the bond strength, the molecule will be emitted as a whole. In the atomic combination mechanism (ACM), on the other hand, both constituents receive energy in two relatively independent collisions, and eventually form the molecule at some stage during the ejection process.

In order to judge whether the emission of a specific molecule is governed either by the DEM or ACM, several statistical formulations of both mechanisms have been published predicting yields [4,5], energy and angular distributions [6–11] of ejected diatomic molecules from analytical sputtering theory and comparing the results with corresponding experimental data. In particular, the internal energy distribution of the emitted

molecules was suggested to be strongly indicative for the molecule formation process [12]. Hence, detailed calculations of the ro-vibrational population of various sputtered diatomic molecules have been performed which are based on a Monte-Carlo approach using essentially independent statistical space, time and momentum distributions for the two ejected atoms as input parameters [12–16]. In this type of calculations, a major problem arises from the choice of an appropriate potential describing the interaction between the constituent atoms of a candidate molecule. In virtually all models mentioned so far, this potential is taken to be that of the free molecule and, hence, the interaction with the remaining surface atoms is switched off instantaneously during the emission and the atoms are assumed to "hop" from the undisturbed surface into a free molecule potential. Especially in cases where the equilibrium distance at the surface largely differs from that in the free molecule, this "hopping" will lead to huge artificial vibrational excitation and the internal energy of the sputtered molecule will be largely overestimated. As a consequence, we feel that in order to accurately describe the internal state distribution of sputtered molecules, the smooth variation of the interaction potential during the ejection should be taken into account. In principle, this is done by a molecular dynamics simulation (MDS) of the sputtering process provided the potential used allows a proper description of both the solid and the free molecule. At the same time, the use of molecular dynamics rather than Monte Carlo methods automatically yields the spatial and temporal correlation between sputtered atoms and, hence, eliminates the need to introduce artificial correlation parameters into statistical models. Moreover, the division of the dimer formation process into DEM and ACM becomes obsolete in a MD simulation. Consequently, a number of MDS studies were carried out in order to enlight the mechanisms of molecule sputtering [17–26]. In these studies, pairwise additive potentials were exclusively used so far to describe the atom–atom interaction within the solid. These potentials, however, cannot describe the interaction of atoms within the solid and in a free molecule at the same time. As a consequence, the same problems regarding the time dependent interaction potential also inherent in the statistical models are encountered again [27]. Only very recently, many-body potentials constructed by the embedded-atom method (EAM) have been successfully applied to the MDS of sputtering phenomena [28]. It is the objective of the present paper to demonstrate that these potentials also permit a reasonably quantitative description of molecule sputtering. As a model system, the formation of Ag_2-dimers sputtered from (111)-, (110)- and (100)-silver surfaces by normally incident Ar^+-ions of 1 keV is studied. First, in order to evaluate the quality of the EAM potential, the total sputter yields, dimer yields as well as the energy distributions of sputtered Ag and Ag_2 are predicted and compared to corresponding experimental results obtained from a polycrystalline silver target. Then, the internal energy distribution and the resulting ro-vibrational population of sputtered Ag_2 is calculated.

2. Description of the calculation

The molecular dynamics calculations have been discussed in detail elsewhere [28,29]. It is of note for all MD simulations, that the accuracy and reliability of the results depend strongly on the quality of the interaction potential from which the atomic forces are derived. From the studies of Garrison, Winograd and coworkers [28,30–35] it has been definitively shown that the embedded-atom method (EAM) potentials [36–38] are currently the best ones available for use in MD simulations of keV particle bombardment of fcc metals. In the EAM, the potential energy of the ith atom in the lattice is written as $E_i = F[\rho_i = \sum_{j \neq i} \rho_{\text{atomic}}(r_{ij})] + \frac{1}{2}\sum_{i \neq j} \phi(r_{ij})$. In this expression, r_{ij} is the distance between the ith and jth atoms, $\rho_{\text{atomic}}(r_{ij})$ is the electron density at the position of the ith atom due to the jth atom, and ρ_i is the total electron density at the position of the ith atom. The embedding function F is a nonlinear function which is taken not to depend on the source of the electron density. Foiles, Daw and Baskes [38] have fit EAM potentials for the

Group VIII fcc metals. We use their Ag potential for these calculations.

The EAM potential of ref. [38] was modified to include a sufficiently repulsive interaction at small internuclear separations. This is necessary as the original construction of the EAM potential did not take into account any data for close encounters (< 2.0 Å) of the atoms. There are undoubtedly numerous ways to proceed but we have chosen the following. For small internuclear separations the interaction should be almost pairwise. Therefore we adjust only the pair portion, $\phi(r_{ij})$, to be more repulsive and, hence, the many-body character of the potential is not affected. We connected the EAM $\phi(r)$ to a Moliere potential [39] at distances between 0.9 and 1.9 Å by use of a cubic spline. Thus for distances greater than 1.9 Å the original EAM pair potential was used. Of note is that the predicted Ag_2 dimer equilibrium distance of 2.4 Å and the nearest neighbour spacing in the solid of 2.9 Å are both considerably larger than the position of the spline point. For the Moliere potential (distances less than 0.9 Å) we chose to use the screening radius of O'Connor and MacDonald [40]. They propose that the Firsov screening radius be multiplied by a factor f, where $f = 0.69 + 0.0051(Z_1 + Z_2) = 1.17$ for Ag–Ag interactions with $Z_1 = Z_2 = 47$. The spline points were chosen so that both the potential and the force were smooth. Of note is that the embedding function is small for these internuclear separations so the net interaction potential is the EAM potential for the attractive regions where many-body effects are important and a Moliere potential at small internuclear separations.

Describing the interaction between two isolated atoms (i.e., a gas phase dimer), the EAM potential (which in this case reduces to a pair potential) can be approximated by a Morse function

$$V_{\mathrm{Morse}}(r) = D_e[1 - e^{-\beta(r-r_e)}]^2 F(r),$$

being truncated by the cut-off function

$$F(r) = \exp[-(r - r_{\mathrm{cut}})/\delta],$$

with $r_{\mathrm{cut}} = 3.45$ Å and $\delta = 0.812$ Å. The parameters D_e, β and r_e are determined by the original EAM fitting procedure and listed in table 1. These values can now be employed to judge whether the EAM provides a reasonable description of a gas phase Ag_2 dimer by comparing them to the corresponding spectroscopic data for Ag_2 also given in table 1. One immediately finds that while β and r_e are virtually identical, the dimer dissociation energy D_e is overestimated by the EAM potential. The implications of this will be discussed later.

Table 1
Morse potential parameters and spectroscopic constants for the spectroscopic and EAM dimer potential

Potential	r_e (Å)	β (Å^{-1})	D_e (eV)	ω_e (cm^{-1})	$\omega_e x_e$ (cm^{-1})
Spectrosc.	2.47 [a]	1.48	1.66 [a]	192.4 [a]	0.643 [a]
EAM	2.43	1.42	2.64	231.4	0.630

[a] Taken from ref. [44].

In order to identify sputtered dimers, the procedure given in ref. [19] was adopted, i.e., the list of atoms sputtered for a given primary ion impact was examined for bound atom pairs. A dimer was identified if exactly one bond was detected for each constituent atom. A pair of atoms was considered to be bound if its internal energy was less than D_e. The internal energy was obtained from the relative kinetic energy E_{rel} and the EAM interaction potential $V(r)$ by

$$E_{\mathrm{int}} = E_{\mathrm{rel}} + V(r),$$

where E_{rel} and V were calculated from the coordinates $\boldsymbol{r}_1$, $\boldsymbol{r}_2$ and velocities $\boldsymbol{v}_1$, $\boldsymbol{v}_2$ of the constituent atoms by

$$E_{\mathrm{rel}} = \frac{\mu}{2} \cdot [\boldsymbol{v}_1 - \boldsymbol{v}_2]^2 \text{ and } V(r) = V(|\boldsymbol{r}_1 - \boldsymbol{r}_2|).$$

Here, μ denotes the reduced mass of the atom pair, r the internuclear separation and L the angular momentum given by

$$L = \mu \cdot |(\boldsymbol{v}_1 - \boldsymbol{v}_2) \times (\boldsymbol{r}_1 - \boldsymbol{r}_2)|.$$

For a given dimer, the quantization of rotational and vibrational energy was done as follows. First, the rotational quantum number N was obtained from L by

$$L^2 = \hbar^2 N'(N' + 1),$$

rounding the resulting N' to the nearest integer N. Then, the turning points $r_{1,2}$ in the effective potential

$$U(r) = V(r) + \frac{L^2}{2\mu r^2}$$

were calculated from

$$E_{\text{int}} - U(r_j) = 0.$$

The vibrational quantum number v was determined using the WKB-approximation

$$v' = -\frac{1}{2} + \frac{1}{\pi\hbar}\int_{r_1}^{r_2}\left[2\mu(E_{\text{int}} - U(r))\right]^{1/2} \mathrm{d}r$$

and again rounding v' to the nearest integer v.

A number of 1000 trajectories were run for each of the three low index fcc crystal faces under investigation. The impact points were chosen to be uniformly distributed over the smallest irreducible surface cell which is a triangle for the (100)- and the (111)- and a rectangle for the (110)-surface.

3. Results and discussion

3.1. Evaluation of the simulation

As a first check of the simulation, the total sputtering yields were calculated for bombardment of (111)-, (110)- and (100)-silver surfaces with normally incident Ar^+ ions. The results are presented in table 2. For comparison with our experimental data which was measured exclusively on polycrystalline samples, we will in the following generally average over the results calculated for the three different crystal faces and assume the mean value to be representative for a polycrystalline surface. Doing so for the total sputter yields gives $\bar{Y}_{\text{tot}} = 4.66$ in good agreement with the experimental value of 4.5 [41]. Determining the absolute yield Y_{Ag_2} of sputtered Ag_2 molecules, we obtain the values which are also displayed in table 2. Due to the fact that the EAM potential overbinds the silver dimers, these numbers are presumably too large. In order to estimate the significance of this effect, we determine the fraction γ of sputtered Ag_2 molecules which are spectroscopically stable, i.e., which possess an internal energy less than the spectroscopic dissociation energy of Ag_2. Evaluation of γ yields values around 75% for all three crystal faces which were then used to correct the calculated dimer yields. The resulting values are labeled "corr" in table 2. In order to compare with experimental results, we calculate the ratio between the numbers of sputtered atoms and dimers by

$$\frac{Ag_2}{Ag} = \frac{Y_{Ag_2}}{Y_{\text{tot}} - \sum_n nY_{Ag_n}}. \tag{1}$$

Here, the sum in the denominator accounts for the formation of Ag_2 dimers as well as multimers Ag_n with $n \geq 3$. The corresponding multimer yields Y_{Ag_n} entering eq. (1) were extracted from the calculated data as described in detail in various publications [17–26]. The resulting dimer/

Table 2
Total sputtering yield Y_{tot}, dimer yield Y_{Ag_2} and dimer/atom ratio calculated for bombardment of three different single crystal silver surfaces with normally incident Ar^+ ions of 1 keV; meaning of the index "corr" see text; the experimental data were taken on a polycrystalline silver surface

Crystal face	Y_{tot}	Y_{Ag_2}	$Y_{Ag_2}^{\text{corr}}$	Ag_2/Ag (%)	Ag_2/Ag^{corr} (%)
(111)	4.495	0.379	0.297	11.3	8.5
(110)	4.146	0.269	0.194	7.9	5.5
(100)	5.346	0.459	0.333	11.8	8.0
Average	4.66	0.369	0.275	10.3	7.3
Experiment	4.5 [a]			7.3 [b]	7.3 [b]

[a] Taken from ref. [41].
[b] Taken from ref. [42].

atom ratios are shown in table 2. Although the values differ drastically from one crystal face to another, the variation is found to be significantly different from that calculated in ref. [18]. We attribute this difference to the many body character of the interaction potential employed in the present study (in contrast to additive pair potentials being used in ref. [18]). The average Ag_2/Ag displayed also in table 2 is calculated to be approximately 30% above an experimental value measured in our laboratory [42] which is also included in the table. If the corrected values of Y_{Ag_2} are introduced into eq. (1), however, a perfect agreement is found between theory and experiment.

In addition to sputtering yields, the energy distribution of sputtered atoms has been shown to represent a critical test for the interaction potential used in the simulation [28]. Fig. 1 depicts the angle integrated energy distribution $N_{Ag}(E)$ calculated for sputtered Ag atoms averaged over the three different crystal faces. As mentioned above, we take these data to be representative for a polycrystalline surface and compare them with an experimental curve measured on our energy resolved SNMS system described

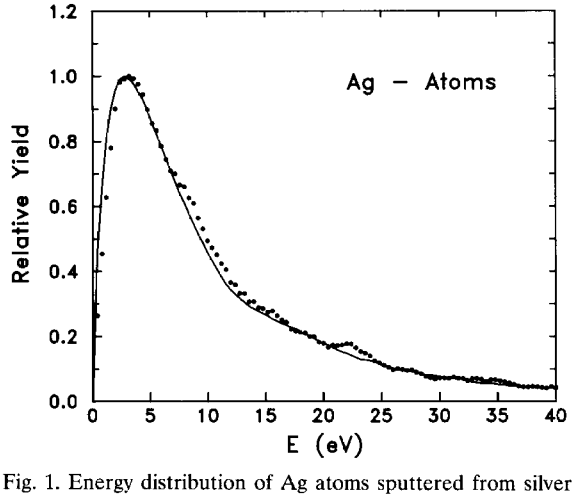

Fig. 1. Energy distribution of Ag atoms sputtered from silver under bombardment with normally incident Ar^+ ions of 1 keV. Data points: calculated for (111)-, (110)- and (100)-surface and averaged. Solid line: measured on a polycrystalline silver surface.

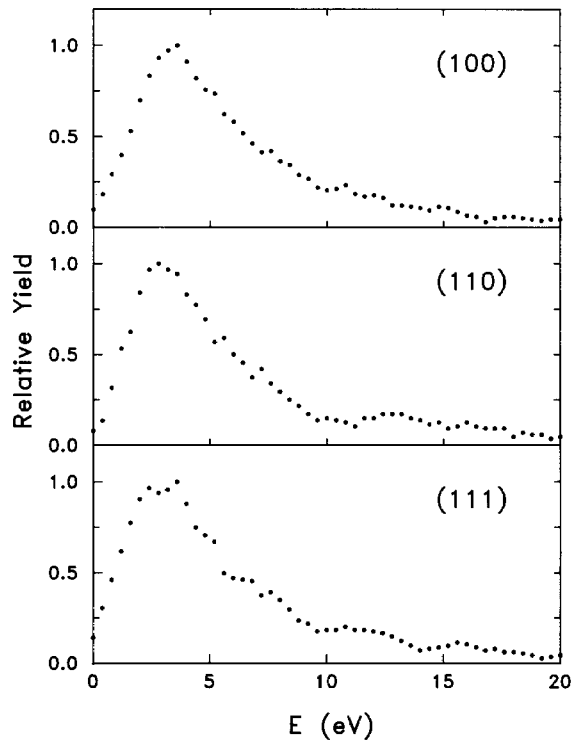

Fig. 2. Calculated energy distributions of Ag_2 dimers sputtered from three low index silver surfaces by normally incident Ar^+ ions of 1 keV.

elsewhere [10,11]. As seen from the figure, excellent agreement is found between simulation and experiment which strongly supports the validity of the EAM potential used for the present simulation. Fig. 2 shows the angle integrated translational energy distribution calculated for Ag_2 dimers sputtered from a (111)-, (110)- and (100)-silver surface, respectively. Apparently the energy distributions calculated for different crystal faces are very similar. The average ejection energy (listed in table 3) is found to be highest for the (110)-, intermediate for the (100)- and lowest for the (111)-surface. Fig. 3 displays the calculated dimer translational energy distribution after averaging over the three crystal faces. For comparison, the corresponding experimental curve determined on polycrystalline silver is included in the figure. Again, apart from a slight energy shift between both distributions by approximately 0.4

Table 3
Average translational energy E^{av}, internal energy E_{int}^{av} as well as vibrational and rotational temperature T_{vib} and T_{rot} calculated for Ag_2 dimers sputtered from three low index single crystal silver surfaces under bombardment with normally incident Ar^+ ions of 1 keV

Crystal face	E^{av} (eV)	E_{int}^{av} (eV)	T_{vib} (K)	T_{rot} (K)
(111)	6.65	1.13	4233	8506
(110)	7.37	1.35	5796	12278
(100)	7.27	1.22	4822	9668

eV (which is of the same order as the uncertainty of the experimental energy zero), good agreement is found between the experimental and simulated data.

As a consequence of this section, we conclude that the present MD simulation represents a good approximation to the experimental data available on sputtering of silver atoms and dimers. In connection with the results of Garrison, Winograd and co-workers [28,30–35], this indicates that the EAM provides a reasonable potential describing the particle interaction during the sputtering process. Hence, in the following section we will extend the calculation towards internal energies of sputtered Ag_2 dimers for which no experimental data exist so far.

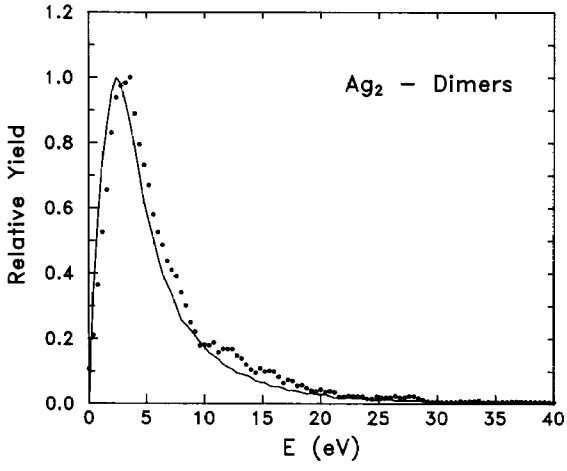

Fig. 3. Energy distribution of Ag_2 dimers sputtered from silver under bombardment with normally incident Ar^+ ions of 1 keV. Data points: calculated for (111)-, (110)- and (100)-surface and averaged. Solid line: measured on a polycrystalline silver surface.

3.2. Internal energies of sputtered dimers

As described in section 2, the total internal energy E_{int} of a sputtered dimer is calculated from the positions and momenta of the constituent atoms at the end of the trajectory integration. Fig. 4 depicts the resulting distribution of E_{int} as evaluated for the three crystal faces. From fig. 4 and the corresponding values listed in table 3 it is clearly seen that the average internal energy is largest for those dimers sputtered from the (110)-surface and lowest for those sputtered from the (111)-surface. Splitting E_{int} into fractions of potential and relative kinetic energy (at the particular time where the trajectory integration was stopped), we find that E_{pot} contributes as much to be total internal energy as E_{rel} and must therefore be accounted for properly in a theoretical description of molecule sputtering. This, however, represents a severe problem in-

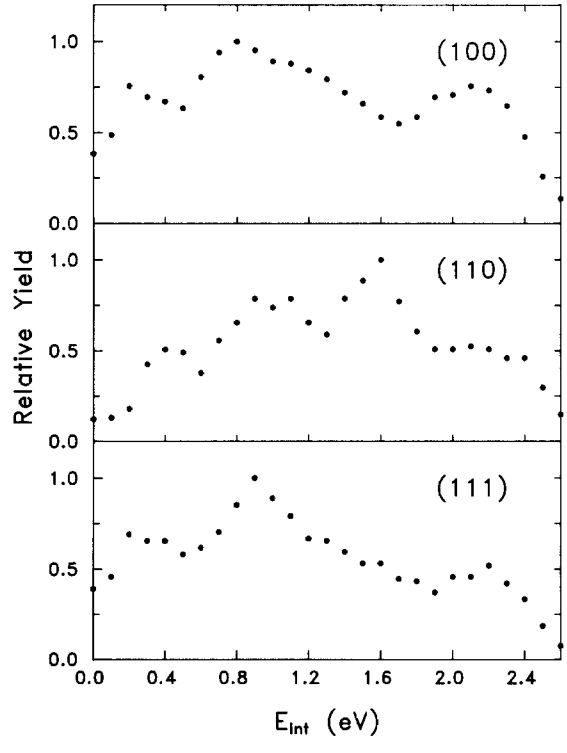

Fig. 4. Distribution of internal energy calculated for Ag_2 dimers sputtered from three low index silver surfaces by normally incident Ar^+ ions of 1 keV.

herent in any statistical model for the formation of sputtered dimers. Since in this type of models the constituent atoms are always considered to pass the surface energy barrier instantaneously at a time t_0, the choice of the appropriate internuclear distance $r_0 = r(t_0)$ and interaction potential $V(r)$ for $t > t_0$ becomes critical. In ref. [8], all sputtered dimers are assumed to be formed with their equilibrium internuclear separation r_e. Our calculations show that this assumption is certainly too rigorous. In a more sophisticated Monte Carlo approach, Snowden et al. [12] assumed a probability distribution of r_0 which depends on the nature of the bombarded surface. For the case of single crystalline samples, they argue that this distribution should be described by weights for nearest, next nearest etc. neighbour distances. Then, however, it immediately follows that according to the Monte Carlo model no dimer ejected from such a surface could possess an internal energy less than $V(r_{nn})$, r_{nn} being the nearest neighbour distance at the surface. Since for all three silver surfaces studied here $r_{nn} = 2.89$ Å and the corresponding potential energy of an isolated Ag_2 molecule amounts to 0.57 eV (calculated from the EAM potential), this represents a clear contradiction to the results shown in fig. 4. To further demonstrate this discrepancy, we compare the vibrational population predicted from the Monte Carlo model with our present results. Fig. 5 depicts the rotationally integrated vibrational population distribution calculated for Ag_2 dimers sputtered from the three single crystal silver surfaces. It is seen that in each case the vibrational population simulated by the MDS can be well described by a Boltzmann distribution. A similar vibrational population was found in an earlier MDS study of Cu_2 dimers sputtered from Cu(111) by low energy O^+ ions [26] yielding a vibrational temperature of 850 K. Also stated in ref. [26], however, one finds that previous unpublished studies of the Cu_2 ejection always yielded non-Boltzmann vibrational distributions. The vibrational temperatures extracted from the least square fits displayed in fig. 5 are listed in table 3. Apparently the dimers ejected from the (110)-surface are significantly "hotter" than those sputtered from the (100)- and the (111)-surface. The

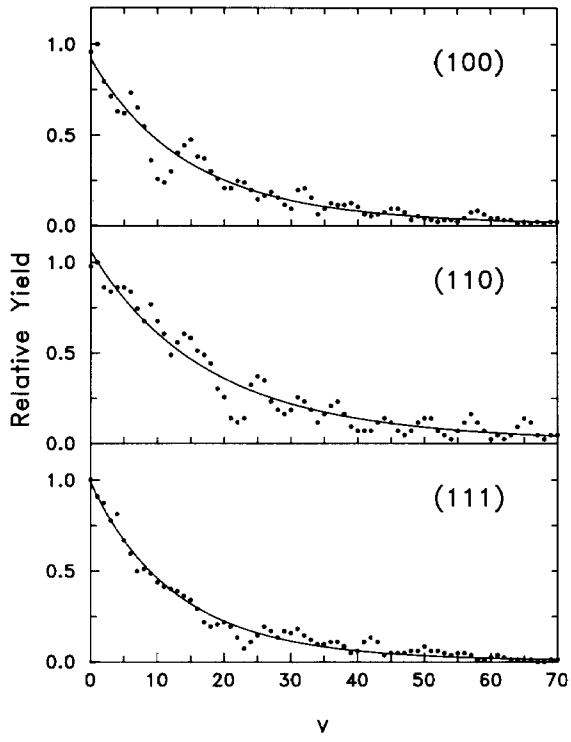

Fig. 5. Vibrational population distribution calculated for Ag_2 dimers sputtered from three low index silver surfaces by normally incident Ar^+ ions of 1 keV. Solid line: least-squares fit corresponding to thermal population.

vibrational temperatures calculated here for sputtered Ag_2 dimers are significantly higher than the temperatures determined experimentally for sputtered K_2, Na_2, Cs_2 [43] and S_2 [15,16]. In contrast to the results shown in fig. 5, the Monte Carlo model would predict a strongly non-thermal vibrational population with a minimum vibrational quantum number around $v_{min} = 28$ (as demonstrated in ref. [13] for the case of sputtered Au_2). We attribute this finding to an artifact inherent in the Monte Carlo simulation which is due to the instantaneous switching from a "bulk" potential governing the interaction of the ejected atoms with their solid state environment to a "vacuum" potential used to identify the sputtered dimer. Such artifacts are always to be expected if the equilibrium distances between the atoms at the surface and within the isolated molecule do not match. They can only be circumvented if the *same* interaction potential is used to

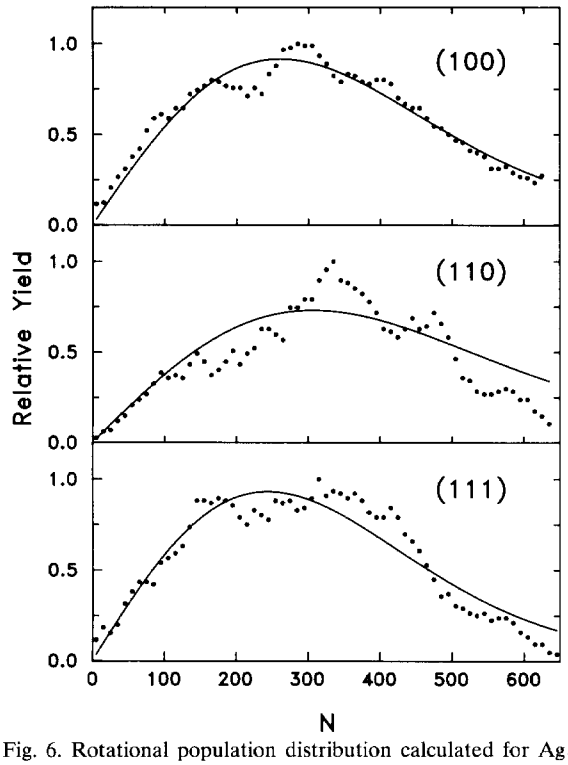

Fig. 6. Rotational population distribution calculated for Ag_2 dimers sputtered from three low index silver surfaces by normally incident Ar^+ ions of 1 keV. Solid line: least-squares fit corresponding to thermal population.

describe both the solid and the isolated dimer, since only in this case the smooth variation of the potential parameters during the ejection can be accounted for.

Fig. 6 shows the rotational population distribution calculated for the different crystal faces. Each data point displayed for a specific rotational quantum number N represents the sum of the population calculated for rotational quantum numbers between $N-5$ and $N+5$. In addition, due to the limited statistics of the calculation, the population was integrated over all vibrational quantum numbers v. From the data displayed in fig. 6, it is apparent that, in agreement with corresponding results from the Monte Carlo model [13] and from previous MDS studies [25,26], the rotational distribution of sputtered Ag_2 dimers is very broad. Included in the figure are least-squares fits assuming thermal population distributions. The resulting rotational temperatures which are listed in table 3 differ markedly between different single crystal surfaces. Again, the dimers sputtered from the (110)-surface exhibit the highest and those sputtered from the (111)-surface the lowest rotational temperature T_{rot}. Furthermore, the value of T_{rot} calculated for a given crystal face is approximately twice as high as that of the corresponding vibrational temperature T_{vib}. This result appears to be quite in contrast to published experimental data. While for sputtered K_2, Na_2 and Cs_2 T_{rot} was observed to be essentially equal to T_{vib} [43], the rotational temperature determined for sputtered S_2 is by a factor of 5 lower than the corresponding T_{vib} [15] and by factors between 30 and 40 lower than the values of T_{rot} calculated here. This finding indicates that the mechanism governing the ion bombardment induced ejection of S_2 from amorphous sulphur and Cs_2 targets must be significantly different from the dimer formation processes occuring during sputtering of metals and, in particular, of silver. Regarding the fact that the bond strength of S_2 (4.37 eV) is large compared to its surface binding energy ($\simeq 0.1$ eV) determined from the translational energy distribution of sputtered S_2 [15] [#1], this result is not surprising since one would expect S_2 to be a typical candidate for the direct emission process described above. For the silver dimers investigated here, on the other hand, the bond strength is smaller than the surface binding energy (as evaluated to be approximately 5 eV from the energy distribution presented in fig. 3) and therefore the formation of these molecules by direct emission is highly improbable.

4. Conclusion

It is shown that by a molecular dynamics simulation using a many-body embedded-atom interaction potential the total yields as well as the translational and internal energy distributions of sputtered dimers can be predicted. From the

[#1] It has been suggested that the most probable energy of sputtered particles should be roughly equal to the half of their surface binding energy [45].

calculations, significant differences have been found between Ag_2 dimers sputtered from different single crystal silver surfaces. The highest average internal energy, corresponding to the highest vibrational and rotational temperatures, have been obtained for the (110)-surface. At the same time, the translational energy distribution of the sputtered dimers calculated for this surface exhibits the highest average kinetic energy of the ejected molecules. On the other hand, the lowest average internal and translational energy as well as the lowest vibrational and rotational temperatures are found for dimers ejected from the (111)-surface. Interestingly, the average ejection energy calculated for sputtered *atoms* is found to be lowest (13.3 eV) for the (110)-, intermediate (14.1 eV) for the (100)- and highest (15.3 eV) for the (111)-surface. Hence, the variation between different crystal faces observed for the average internal and translational energy of the sputtered dimers cannot be explained by the simple mechanism that "hotter" molecules are formed by "faster" atoms. A correspondence of this type, however, would be expected from purely kinematical molecule formation models like the one proposed in ref. [8], which are based on phase space considerations alone and neglect the potential energy stored in the interaction between the constituent atoms. On the other hand, the mean internal energy as well as the population temperatures appear to be ordered in the same way as the mean internuclear distance between the surface atoms which is largest for the (110)- and lowest for the (111)- surface. As a consequence, we conclude that an appropriate description of the intramolecular interaction *during the ejection process* represents a necessary prerequisite in order to quantitatively understand the formation of sputtered molecules. Using the embedded-atom interaction potential, such a description can be provided by molecular dynamics simulations, whereas it appears to be quite problematic in statistical models.

Acknowledgements

The authors wish to express their thanks to Ms. Claudia Mössner for technical assistance with the computations. Thanks are also due to the Deutsche Forschungsgemeinschaft for financial support within the Sonderforschungsbereich 91.

References

[1] H. Oechsner, in: Physics of ionized gases 1984, Eds. M. Popovic and P. Krstic (World Scientific, Singapore, 1985) p. 571.
[2] H.M. Urbassek, Nucl. Instrum. Methods B 18 (1987) 587, and Habilitationsschrift, University of Braunschweig (1989).
[3] A.E. de Vries, Nucl. Instrum. Methods B 27 (1987) 173.
[4] W. Gerhard, Z. Phys. B 22 (1975) 31.
[5] H. Oechsner, H. Schoof and E. Stumpe, Surf. Sci. 76 (1978) 343.
[6] G.P. Können, A. Tip and A.E. de Vries, Rad. Eff. 21 (1974) 269; 26 (1975) 23.
[7] R.A. Haring, H.E. Roosendaal and P.C. Zalm, Nucl. Instrum. Methods B 28 (1987) 205.
[8] R. Hoogerbrugge and P.G. Kistemaker, Nucl. Instrum. Methods B 21 (1987) 37.
[9] K.J. Snowdon and R.A. Haring, Nucl. Instrum. Methods B 18 (1987) 596.
[10] A. Wucher and H. Oechsner, Nucl. Instrum. Methods B 18 (1987) 458.
[11] J. Dembowski, Thesis, University of Kaiserslautern (1986).
[12] K.J. Snowdon, R. Hentschke, W. Heiland and P. Hertel, Z. Phys. A 318 (1984) 261.
[13] K.J. Snowdon, B. Willerding and W. Heiland, Nucl. Instrum. Methods B 14 (1986) 467.
[14] P. Sigmund, H.M. Urbassek and D. Matagrano, Nucl. Instrum. Methods B 14 (1986) 495.
[15] R. de Jonge, T. Baller, M.G. Tenner, A.E. de Vries and K.J. Snowdon, Europhys. Lett. 2 (1986) 499; Nucl. Instrum. Methods B 17 (1986) 213.
[16] R. de Jonge, K.W. Benoist, J.W.F. Majoor and A.E. de Vries, Nucl. Instrum. Methods B 28 (1987) 214.
[17] D.E. Harrison, Jr. and C.B. Delaplain, J. Appl. Phys. 47 (1976) 2252.
[18] N. Winograd, D.E. Harrison, Jr. and B.J. Garrison, Surf. Sci. 78 (1978) 467.
[19] B.J. Garrison, N. Winograd and D.E. Harrison, Jr., J. Chem. Phys. 69 (1978) 1440.
[20] B.J. Garrison, N. Winograd and D.E. Harrison, Jr., Phys. Rev. B 18 (1978) 6000.
[21] N. Winograd, K.E. Foley, B.J. Garrison and D.E. Harrison, Jr., Phys. Lett. A73 (1979) 253.
[22] N. Winograd, B.J. Garrison, T. Fleisch, W.N. Delgass and D.E. Harrison, Jr., J. Vac. Sci. Technol. 16 (1979) 629.
[23] S.P. Holland, B.J. Garrison and N. Winograd, Phys. Rev. Lett. 44 (1980) 756.
[24] B.J. Garrison, J. Am. Chem. Soc. 102 (1980) 6553.

[25] N. Winograd, B.J. Garrison and D.E. Harrison, Jr., J. Chem. Phys. 73 (1980) 3473.
[26] D.E. Harrison, Jr., P. Avouris and R. Walkup, Nucl. Instrum. Methods B 18 (1986) 349.
[27] H.H. Andersen, Nucl. Instrum. Methods B 18 (1987) 321.
[28] B.J. Garrison, N. Winograd, D.M. Deaven, C.T. Reimann, D.Y. Lo, T.A. Tombrello, D.E. Harrison, Jr. and M.H. Shapiro, Phys. Rev. B 37 (1988) 7197.
[29] D.E. Harrison, Jr., CRC Critical Reviews of Solid State and Materials Sciences 14 (1988) S1.
[30] D.Y. Lo, T.A. Tombrello, M.H. Shapiro, B.J. Garrison, N. Winograd and D.E. Harrison, Jr., J. Vac. Sci. Technol. A 6 (1988) 708.
[31] C.T. Reimann, K. Walzl, M. El-Maazawi, D.M. Deaven, B.J. Garrison and N. Winograd, J. Chem. Phys. 89 (1988) 2539.
[32] C.T. Reimann, M. El-Maazawi, K. Walzl, B.J. Garrison, N. Winograd and D.M. Deaven, J. Chem. Phys. 90 (1989) 2027.
[33] J. Garrison, K. Walzl, M. El-Maazawi, N. Winograd, C.T. Reimann and D.M. Deaven, J. Rad. Eff. Defects Solids 109 (1989) 287.
[34] C.T. Reimann, K. Walzl, M. El-Maazawi, B.J. Garrison and N. Winograd, Secondary Ion Mass Spectrometry SIMS VI, Eds. A. Benninghoven, A.M. Huber and H.W. Werner (Wiley & Sons, Chichester, 1988).
[35] R. Maboudian, Z. Postawa, M. El-Maazawi, B.J. Garrison and N. Winograd, Phys. Rev. B 42 (1990) 7311.
[36] M.S. Daw and M.I. Baskes, Phys. Rev. Lett. 50 (1983) 1285.
[37] M.S. Daw and M.I. Baskes, Phys. Rev. B 29 (1984) 6443.
[38] S.M. Foiles, M.I. Baskes and M.S. Daw, Phys. Rev. B 33 (1986) 7983.
[39] I.M. Torrens, Interatomic Potentials (Academic Press, New York, 1972).
[40] D.J. O'Connor and R.J. MacDonald, Rad. Eff. 34 (1977) 247.
[41] H. Oechsner, Z. Phys. 261 (1973) 37.
[42] K. Franzreb, A. Wucher and H. Oechsner, Fresenius, J. Anal. Chem., in press.
[43] P. Fayet, J.P. Wolf and L. Wöste, Phys. Rev. B 33 (1986) 6792.
[44] M.D. Morse, Chem. Rev. 86 (1986) 1049.
[45] M.W. Thompson, Philos. Mag. 18 (1968) 377.